

Enhanced photocatalytic activity of transparent carbon nanowall/TiO₂ heterostructures

Mattia Pierpaoli^{1,a)}, Aneta Lewkowicz², Michał Ryciewicz¹, Karol Szczodrowski², Maria Letizia Ruello³ and Robert Bogdanowicz^{1,b)}

¹*Department of Metrology and Optoelectronics, Faculty of Electronics, Telecommunication and Informatics, Gdańsk University of Technology, Poland*

²*Institute of Experimental Physics, University of Gdansk, Poland*

³*Department of Materials, Environmental Sciences and Urban Planning, Università Politecnica delle Marche, Italy*

Abstract

The synthesis of novel tunable carbon-based nanostructure represented a pivotal point to enhance the efficiency of existing photocatalysts and to extend their applicability to a wider number of sustainable processes.

In this letter, we describe a transparent photocatalytic heterostructure by growing boron-doped carbon nanowalls (B-CNWs) on quartz, followed by a simple TiO₂ sol-gel deposition. The effect on the thickness and boron-doping in the B-CNWs layer was studied, and the photocatalytic removal of nitrogen oxides (NO_x) measured.

Our results show that TiO₂, in the anatase form, was uniformly deposited on the carbon nanowall layer. The underlying carbon nanowall layer played a double role in the heterostructure: it both affects the crystallinity of the TiO₂ and promotes the separation of the photoexcited electron-holes, by increasing the number of contact points between the two layers. In summary, the combination of B-CNWs with TiO₂ can enhance the separation of the electron-hole photogenerated charges, due to the peculiar CNWs maze-like structure.

Keywords

TiO₂, carbon nanowalls, carbon materials, nanocomposites

1. Introduction

Boron-doped carbon nanowalls (B-CNWs) are open boundary, vertically-oriented, graphene sheets that are only a few layers thick [1,2]. B-CNWs attract attention thanks to their tunable band gap, high conductivity, high mechanical robustness, and high light absorption. To achieve a particular morphology and characteristic, it is possible to vary the synthesis parameters, such as the boron-doping level, synthesis temperature, plasma intensity, substrate material, deposition time, and gas precursor [3].

The formation of the electron/hole couple on the titanium dioxide (TiO₂) surface induces the formation of active species which take part in the oxidative process. However, the enhancement of the photocatalytic efficiency of TiO₂ is still of current interest, because of the low quantum yield caused by the rapid recombination of photogenerated electrons and holes.

Various allotropes of carbon materials, including activated carbon [4,5], carbon nanotubes [6], carbon nanofibres, carbon quantum dots and graphene [7,8], have been employed to realise TiO₂ composites, with the aim of enhancing the photocatalytic activity, by slowing the recombination of photogenerated electron-hole pairs due to a semiconductor-semiconductor junction and extending the excitation wavelength [6,9]. To date, only one attempt by Wang et al. is reported in the literature to realise a TiO₂/CNW composite [10]. Moreover, the possibility of doping the carbon nanowall with boron allows a further degree of freedom to be added in creating a carbonaceous substrate having a predetermined band gap and electrical conductivity.

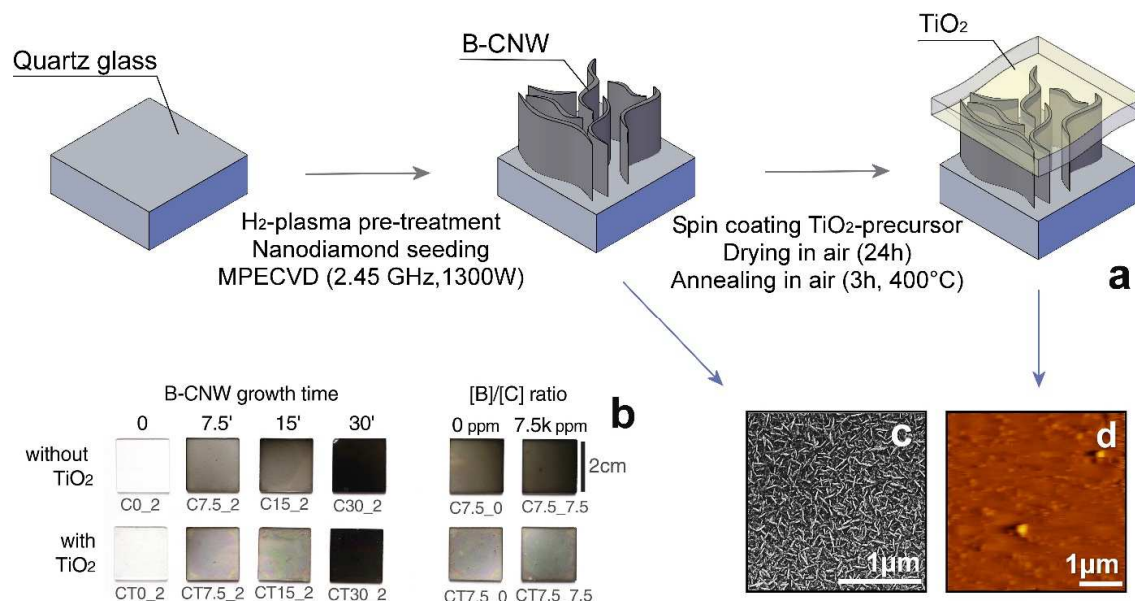


Fig. 1. (a) Fabrication of the samples (b) Picture of the samples, (c) SEM picture of the B-CNW layer (C30_2); (d) AFM image of TiO₂ film (CT30_2).

In this Letter, we report the realisation of a transparent B-CNWs/TiO₂ heterostructure, exhibiting enhanced photocatalytic activity toward nitrogen oxide (NO) removal. TiO₂ was deposited, by a simple sol-gel technique, on B-CNWs grown by microwave-plasma enhanced chemical vapour deposition (MPCVD) on fused quartz glass. The amount of boron doping was varied to vary the layer thickness of the CNWs and B-CNWs, in order to study the impact on the optical and photocatalytic properties. To the best of our knowledge, this is the first study about a transparent heterostructure in which TiO₂ was deposited by sol-gel on boron-doped carbon nanowalls.

2. Experimental

A schematic of the experimental procedure is reported in Fig.1a. B-CNWs were synthesised by MPCVD (SEKI Technotron AX5400S, 2.45 GHz, 1300W) with a gas mixtures of H₂, CH₄, B₂H₆, and N₂, at a pressure of 50 Torr and the substrate holder was heated to 700°C. 2x2 cm pieces of quartz glass were pre-treated with a hydrogen-rich plasma, before being seeded by spin-coating in a diamond slurry [11].

The precursor solution for TiO₂ thin films was obtained using titanium(IV) tetra(2-propanolate), propan-2-ol, Triton X-100 and hydrochloric acid. The detailed procedure on sol preparation can be found in our earlier works [12,13]. Thin films were distributed over the B-CNW using the spin-coating technique, dried in air for 24 h and annealed for 3 h at 400°C. The temperature was chosen as a compromise between developing a TiO₂-crystalline structure without initiating B-CNW combustion (supplementary material).

3. Results and discussion

Pictures of the samples are reported in Figure 1b. The B-CNWs' lengths range within tens and hundreds of nanometres[3], with a layer thickness ranging from 45 to 160nm, respectively, for samples grown for 7.5 and 30 mins. Differently from the composite prepared by Wang et al. [10], the heterostructure exhibit an extremely low surface roughness, in the order of tens of nanometers, attributable to the annealed TiO₂ layer (Fig.1d and supplementary material).

The carbonaceous nanostructured substrate characteristics are reported in Fig.2a-b. The value of transmittance of the B-CNW-only sample at 365nm, a value which was chosen based on the TiO₂ band gap, decreases with increasing B-CNW thickness. The increase of the B-CNW thickness led to a well-developed network, with longer nanowalls and enhanced electrical conductivity[17], while boron doping affect less the B-CNWs morphology. All heterostructures present high absorbance in the ultraviolet, while the process duration strongly affects the transmittance across the whole UV-visible spectrum (supplementary material). From the XRD results, the strong

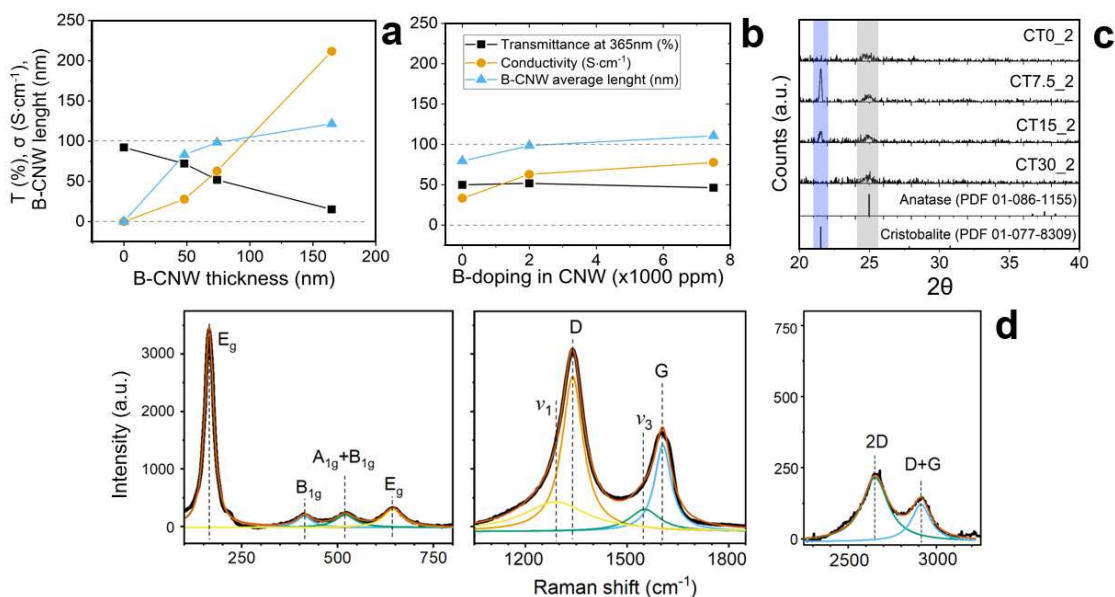


Fig. 2 – (a-b) Optical transmittance at 365nm, electrical conductivity and average nanowall length for the B-CNWs-only samples; (c) XRD diffractogram for the different composites; (d) Deconvolution of the Raman spectrum for the representative CT15_2 sample

diffraction peak at $2\theta=24.95^\circ$, reported in Fig. 2c, can be attributed to the most intense reflection of the crystalline anatase phase, and the broad peak suggests that the average diameter is in the nanometre scale. The intensity of the anatase phase is the same with increasing B-CNW thickness, because of its dependence on the crystallite size and porosity structure. A second peak, at $2\theta=22^\circ$, due to the high-temperature treatment on the quartz substrate, is related to the presence of cristobalite.

A deconvoluted Raman spectrum of the representative sample CT15_2, with labelled peaks, is reported in Fig. 2c. A well-resolved TiO_2 Raman peak is observed at 157cm^{-1} for the TiO_2 and at around 163cm^{-1} for the $\text{TiO}_2/\text{B-CNWs}$ samples, which is attributed to the main anatase vibrational mode, followed by peaks at about 413cm^{-1} , 526cm^{-1} and 645cm^{-1} . The other two main bands at $\sim 1560\text{cm}^{-1}$ and $\sim 1340\text{cm}^{-1}$ are attributed to the G and D band of the carbon nanowall, respectively [14].

A shift of the main peak position toward the higher energy side and an intensification of the full width at half maximum (FWHM) of the main anatase mode, was attributed to the phonon confinement (with decreasing grain size) or to the presence of internal stresses[15]. In our study, the blueshift appearing in the TiO_2 -only sample (CT0_2) is due to the small crystallite size (Table 1), as confirmed by the AFM and XRD results, and it is comparable to what is reported in the literature[15,16]. The presence of the underlying B-CNWs induces additional stresses in the anatase structure, independently of the thickness, due to the nanowalls' contrasting action during calcination, which results in an additional E_{1g} peak shift and FWHM increase. This aspect is better highlighted when the principal Raman mode is compared with the average B-CNW length and projected area. These two parameters were obtained by segmentation of SEM analysis (using Gwyddion 2.54, details are reported in the supplementary materials) and are representative of the nanowall density and morphology. The results, reported in Table 1, point out a positive correlation between the anatase internal stress and the morphology of the underlying B-CNW substrate.

Table 1 – Morphology of the B-CNWs and resultant E_{1g} mode of the overlying TiO_2 .

| Sample | B-CNWs | | TiO_2 | | E_g (eV) |
|---------|-------------------------|-----------------------|---|---------------------------------------|---------------|
| | Mean grain size (nm) | Projected area (%) | E_{1g} position (cm^{-1}) | E_{1g} FWHM (cm^{-1}) | |
| CT0_2 | 0 | 0 | 157 | 17.7 | 3.46 |
| CT7.5_2 | 40 | 37 | 164 | 27.6 | 3.44 |
| CT15_2 | 33 | 35 | 164 | 27.9 | 3.40 |

| | | | | | |
|----------|----|----|-----|------|------|
| CT30_2 | 26 | 22 | 165 | 30.3 | 3.38 |
| CT15_0 | 17 | 20 | 161 | 22.7 | 3.36 |
| CT15_7.5 | 29 | 35 | 163 | 26.8 | 3.40 |

The photocatalytic performance of the prepared heterostructures was evaluated by photocatalytic oxidation of nitrogen oxide (NO) in a plug-flow reactor, at different flow velocities. The experimental apparatus is schematised in Figure 3a and the reactor details are reported in Figure 3b. The detailed test conditions are reported in supplementary material.

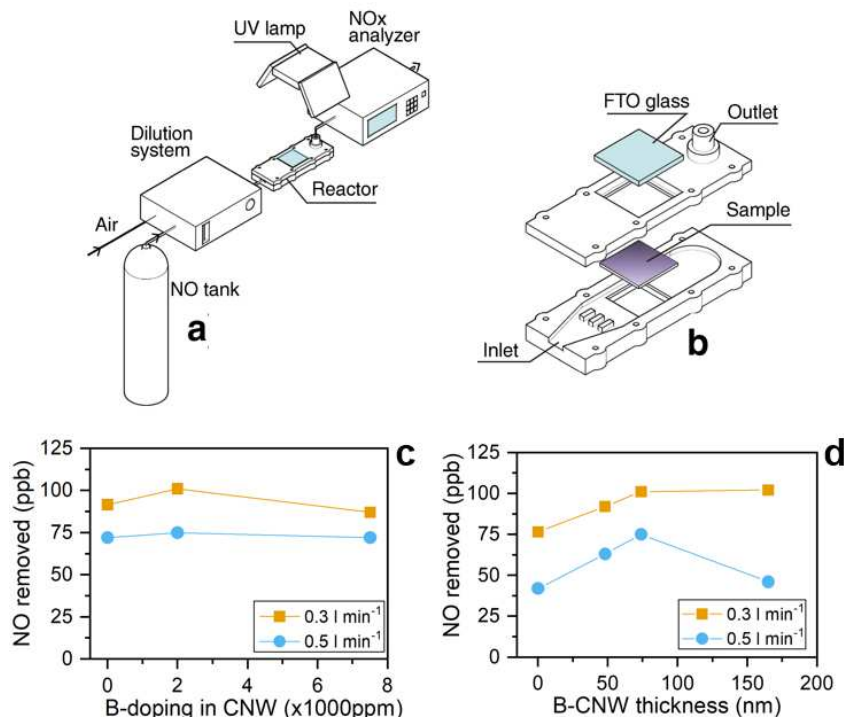


Fig. 3 – (a) Schematic of the apparatus for the photocatalytic test and (b) reactor details. Results of the photocatalytic activity for different (c) boron dopings and (d) B-CNW layer thicknesses.

The prepared heterostructures exhibit an enhanced photocatalytic activity toward the degradation of NO, when compared to the nanocrystalline TiO₂-only. This enhancement depends on the B-CNWs' thickness, as it increases first and then remains constant with further increases in the B-CNWs' thickness; the best efficiency was achieved with a thickness less than 100nm. This aspect, which is reflected by a narrowing of the bandgap, can be better explained with two competitive behaviours:

- a longer B-CNW growing time leads to longer nanowall, therefore to a better-developed structure with enhanced electrical conductivity and to a higher number of contact points between the photocatalyst and the underlying carbon layer [18], which promotes an efficient charge separation;
- the higher absorbance of thicker B-CNW layers limits the amount of light adsorbed by the catalyst, so increases the number of photogenerated electron/hole couples.

A similar behaviour has been reported in the literature for different carbon nanocomposites, such as TiO₂/graphene [19,20] and TiO₂/carbon nanotubes [21]. However, the explanation of the optimal concentration, is not univocal.

4. Conclusion

In summary, a transparent B-CNW/TiO₂ heterostructure with enhanced photocatalytic activity was fabricated. The B-CNW layer affects both the TiO₂ crystalline structure and provides efficient charge separation due to the widespread contact lines. Further studies are intended to optimise the B-CNWs' characteristics to enhance the photocatalyst charge separation and to provide an efficient nanostructured support.

ACKNOWLEDGMENTS

This research is supported by The Polish National Agency for Academic Exchange (NAWA), under the Ulam program, Agreement no. PPN/ULM/2019/1/00061/DEC/1 and by the National Centre for Science and Development [347324/12/NCBR/2017]. The DS funds of the Faculty of Electronics, Telecommunications and Informatics of the Gdansk University of Technology are also acknowledged.

REFERENCES

- [1] M. Sobaszek, K. Siuzdak, J. Ryl, M. Sawczak, S. Gupta, S.B. Carrizosa, M. Ficek, B. Dec, K. Darowicki, R. Bogdanowicz, *J. Phys. Chem. C*. 121 (2017) 20821–20833. <https://doi.org/10.1021/acs.jpcc.7b06365>.
- [2] K. Siuzdak, M. Ficek, M. Sobaszek, J. Ryl, M. Gnyba, P. Niedziałkowski, N. Malinowska, J. Karczewski, R. Bogdanowicz, *ACS Appl. Mater. Interfaces*. 9 (2017) 12982–12992. <https://doi.org/10.1021/acsami.6b16860>.
- [3] M. Pierpaoli, M. Ficek, M. Rycewicz, M. Sawczak, J. Karczewski, M. Ruello, R. Bogdanowicz, *Materials (Basel)*. 12 (2019) 547. <https://doi.org/10.3390/ma12030547>.
- [4] A. Matsumoto, K. Tsutsumi, K. Kaneko, *Langmuir*. 8 (1992) 2515–2520. <https://doi.org/10.1021/la00046a027>.
- [5] M. Pierpaoli, C. Giosuè, M.L. Ruello, G. Fava, *Environ. Sci. Pollut. Res.* 24 (2017) 12638–12645. <https://doi.org/10.1007/s11356-016-7880-x>.
- [6] K. Dai, X. Zhang, K. Fan, P. Zeng, T. Peng, *J. Nanomater.* 2014 (2014) 1–8. <https://doi.org/10.1155/2014/694073>.
- [7] H. Zhang, X. Lv, Y. Li, Y. Wang, J. Li, *ACS Nano*. 4 (2010) 380–386. <https://doi.org/10.1021/nn901221k>.
- [8] Y. Zhang, Z.-R. Tang, X. Fu, Y.-J. Xu, *ACS Nano*. 4 (2010) 7303–7314. <https://doi.org/10.1021/nn1024219>.
- [9] W. Cui, Q. Liu, N. Cheng, A.M. Asiri, X. Sun, *Chem. Commun.* 50 (2014) 9340–9342. <https://doi.org/10.1039/c4cc02713b>.
- [10] H. Wang, X. Quan, H. Yu, S. Chen, *Carbon N. Y.* 46 (2008) 1126–1132. <https://doi.org/10.1016/j.carbon.2008.04.016>.
- [11] M. Sobaszek, K. Siuzdak, J. Ryl, M. Sawczak, S. Gupta, S.B. Carrizosa, M. Ficek, B. Dec, K. Darowicki, R. Bogdanowicz, *J. Phys. Chem. C*. 121 (2017) 20821–20833. <https://doi.org/10.1021/acs.jpcc.7b06365>.
- [12] A. Lewkowicz, A. Synak, B. Grobelna, R. Bogdanowicz, J. Karczewski, K. Szczodrowski, M. Behrendt, *Opt. Mater. (Amst)*. 36 (2014) 1739–1744. <https://doi.org/10.1016/J.OPTMAT.2014.02.033>.
- [13] A. Lewkowicz, P. Bojarski, A. Synak, B. Grobelna, I. Akopova, I. Gryczyński, L. Kułak, *J. Phys. Chem. C*. 116 (2012) 12304–12311. <https://doi.org/10.1021/jp3022562>.
- [14] A.C. Ferrari, J. Robertson, O. Ferrari, J.O.H.N. Robertson, *Philos Trans A Math Phys Eng Sci*. 15 (2004) 2477–512. <https://doi.org/10.1098/rsta.2004.1452>.
- [15] S. Balaji, Y. Djaoued, J. Robichaud, *J. Raman Spectrosc.* 37 (2006) 1416–1422. <https://doi.org/10.1002/jrs.1566>.
- [16] K.-R. Zhu, M.-S. Zhang, Q. Chen, Z. Yin, *Phys. Lett. A*. 340 (2005) 220–227. <https://doi.org/10.1016/j.physleta.2005.04.008>.
- [17] M. Pierpaoli, A. Lewkowicz, M. Ficek, M.L. Ruello, R. Bogdanowicz, *Photonics Lett. Pol.* 10 (2018) 54–56. <https://doi.org/10.4302/plp.v10i2.825>.
- [18] Z. Bo, W. Zhu, W. Ma, Z. Wen, X. Shuai, J. Chen, J. Yan, Z. Wang, K. Cen, X. Feng, *Adv. Mater.* 25 (2013) 5799–5806. <https://doi.org/10.1002/adma.201301794>.
- [19] V. Štengl, D. Popelková, P. Vláčil, *J. Phys. Chem. C*. 115 (2011) 25209–25218. <https://doi.org/10.1021/jp207515z>.
- [20] W. Fan, Q. Lai, Q. Zhang, Y. Wang, *J. Phys. Chem. C*. 115 (2011) 10694–10701. <https://doi.org/10.1021/jp2008804>.
- [21] A.M. Kamil, H.T. Mohammed, A.A. Balakit, F.H. Hussein, D.W. Bahnemann, G.A. El-Hiti, *Arab. J. Sci. Eng.* 43 (2018) 199–210. <https://doi.org/10.1007/s13369-017-2861-z>.